

Thermoacoustic shocks in complex plasmas

A. P. Misra^{1,*} and Gadadhar Banerjee^{1,†}

¹*Department of Mathematics, Siksha Bhavana, Visva-Bharati University, Santiniketan-731 235, West Bengal, India*
(Dated: May 3, 2022)

The formation of thermoacoustic shocks is revealed in a fluid complex plasma. The thermoacoustic wave mode can be damped (or anti-damped) when the contribution from the thermoacoustic interaction is lower (or higher) than that due to the particle collision and/or the kinematic viscosity. In the nonlinear regime, the thermoacoustic wave, propagating with the acoustic speed, can evolve into small amplitude shocks whose dynamics is governed by the Bateman-Burgers equation with nonlocal nonlinearity. The latter can cause the shock fronts to be stable (or unstable) depending on the collision frequency remains below (or above) a critical value and the thermal feedback is positive. The existence of different kinds of shocks and their characteristics are analyzed with the system parameters that characterize the thermal feedback, thermal diffusion, heat capacity per fluid particle, the particle collision and the fluid viscosity. A good agreement between the analytical and numerical results are also noticed.

I. INTRODUCTION

The thermoacoustic instability [1, 2] has its own importance from fundamental points of view as they can cause pulsations leading to particle acceleration in certain environments including those where the combustion reaction takes place [3–5]. Recently, the onset of such instability in complex plasmas has been reported in the linear regime [6, 7]. In Ref. [6], it was shown that the non-reciprocal effective interactions of charged particles can provide positive thermal feedback which, in turn, leads to the amplification of thermoacoustic waves. The theoretical prediction of such instability was also verified experimentally in that work. In another work [7], the thermoacoustic instability has also been studied in the weakly and strongly coupled dusty plasma systems. On the other hand, the formation of thermoacoustic shocks has been experimentally observed in a gas column of a resonance tube with temperature gradient [8, 9]. However, the evolution of thermoacoustic shocks in plasmas has not been investigated so far.

The aim of this work is to revisit the theory thermoacoustic waves, especially in the nonlinear regime, to investigate the generation of thermoacoustic shocks propagating with a velocity close to the acoustic speed and their characteristics in fluid complex plasmas. Our analysis shows that the thermal feedback can indeed induce shock waves and they can be damped or anti-damped depending on the collision frequency below or above a critical value. A qualitative agreement of the analytical and numerical results are also found to justify the existence of different kinds of shocks.

II. FLUID MODEL AND DISPERSION RELATION

The equations describing the generation of acoustic-like waves in one space dimension in a fluid complex plasma with the effects of temperature gradient, thermal feedback, the particle collision and the fluid kinematic viscosity are [6]

$$\frac{\partial \rho}{\partial t} + \frac{\partial}{\partial x}(\rho v) = 0, \quad (1)$$

$$\frac{\partial v}{\partial t} + v \frac{\partial v}{\partial x} = -\frac{1}{\rho} \frac{\partial}{\partial x}(\rho T) - \nu v + \mu \frac{\partial^2 v}{\partial x^2}, \quad (2)$$

$$\frac{\partial T}{\partial t} + v \frac{\partial T}{\partial x} = \chi \frac{\partial^2 T}{\partial x^2} - \frac{2\nu}{\Gamma}(T - 1) + q, \quad (3)$$

where $\rho = nm$ is the fluid mass density normalized by its equilibrium value ρ_0 with n denoting the number density and m the mass, v is the center-of-mass fluid flow velocity normalized by the acoustic speed $c_s = \sqrt{k_B T_0/m}$ with k_B denoting the Boltzmann constant, T is the total thermodynamic temperature normalized by its equilibrium value T_0 , ν is the collision frequency (damping rate) normalized by the plasma oscillation frequency $\omega_p = \sqrt{n_0 Q^2/\epsilon_0 m}$ with Q denoting the particle charge, μ is the coefficient of fluid kinematic viscosity normalized by $\lambda_D^2 \omega_p$ with $\lambda_D = c_s/\omega_p$ denoting the effective Debye length, χ is the coefficient of thermal diffusivity normalized by c_s^2/ω_p , Γ is the heat capacity, and $q(\rho, T)$ is the heat source normalized by $T_0 \omega_p$. Also, the space and time coordinates x and t are normalized, respectively, by λ_D and ω_p^{-1} .

We consider the propagation of compressional waves in plasmas along the x -direction. Assuming that the perturbations of density, velocity, and temperature are small compared to their equilibrium values and they vary as plane waves of the form $\exp(ikx - i\omega t)$ with wave number k and wave frequency ω , and linearizing Eqs. (1)-(3),

* apmisra@visva-bharati.ac.in

† gban.iitkgp@gmail.com

we obtain the following linear dispersion law [6].

$$\left[\omega^2 + i(\nu + \mu k^2)\omega - k^2 \right] \times \left[\omega + i \left(\chi k^2 + \frac{2\nu}{\Gamma} - q_T \right) \right] = i q_\rho k^2 \quad (4)$$

where the parameters $q_T = (\partial q / \partial T)_0$ and $q_\rho = (\partial q / \partial \rho)_0$, calculated at the equilibrium values $T = 1$ and $\rho = 1$, correspond to the thermal feedback of the media to the temperature and density variations. Note that the wave frequency ω (or wave number k) becomes complex due to the effects of the thermal feedback as well as the collisional and the viscosity effects. The dispersion equation (4) agrees exactly with that in Ref. [6] except the term $\propto \mu$ due to the effect of the kinematic viscosity. In absence of the heat source or thermal feedback, i.e., for $q_\rho = q_T = 0$, the thermal mode and the acoustic mode are decoupled for which Eq. (4) gives

$$\omega = -i \left(\chi k^2 + \frac{2\nu}{\Gamma} \right), \quad (5)$$

and

$$\omega = k \sqrt{1 - \frac{(\nu + k^2 \mu)^2}{4k^2}} - i \frac{\nu + k^2 \mu}{2}. \quad (6)$$

Equation (5) corresponds to a purely damped thermal mode whereas Eq. (6) that to an acoustic-like wave with the damping rate $\propto (\nu + \mu k^2)/2$ due to the particle collision and/or the kinematic viscosity provided k lies in a very small interval $1 - a < k < 1 + a$, where $a = \sqrt{1 - \nu\mu}$. This small regime is, however, not of interest and thus inadmissible. So, we look for an acoustic mode with $\omega \simeq k + \delta\omega$, where $\delta\omega$ is a small correction to the wave frequency due to the thermoacoustic interactions. Separating the real and imaginary parts, from Eq. (4) we obtain the following expressions for the real wave frequency and the growth/damping rate.

$$\Re\omega = k \left[1 + \frac{q_\rho}{2} \frac{\chi k^2 + 2\nu/\Gamma - q_T}{k^2 + (\chi k^2 + 2\nu/\Gamma - q_T)^2} \right], \quad (7)$$

$$\Im\omega = -\frac{1}{2}(\nu + \mu k^2) + \frac{q_\rho}{2} \frac{k^2}{k^2 + (\chi k^2 + 2\nu/\Gamma - q_T)^2}. \quad (8)$$

From Eq. (7) it follows that the phase velocity of the thermoacoustic wave is constant, i.e., the wave becomes dispersionless in the long wavelength limit $k \rightarrow 0$. However, as k increases, in contrast to the low-frequency acoustic waves, the phase velocity approaches a constant value (i.e., close to the acoustic speed c_s). On the other hand, from Eq. (8) it is evident that the wave can be stable (damped) or unstable (anti-damped) depending on whether the thermal contribution is smaller or larger than the term associated with the collision and the viscosity. Typically, for positive values of q_ρ and small values

of ν and μ , $\Im\omega$ becomes positive, implying the wave amplitude to grow leading to the thermoacoustic instability [6].

In order to study the characteristics of the wave mode and the growth/decay rate in details, we numerically analyze Eqs. (7) and (8). The results are displayed in Fig. 1. The profiles of $\Re\omega$ are shown in subplots (a) and (c), and those of $\Im\omega$ are in subplots (b) and (d) for different values of the parameters, namely q_ρ and q_T that characterize the thermal feedback; the heat capacity per particle Γ , the coefficient of the thermal diffusivity χ , the collision frequency ν and the coefficient of the kinematic viscosity μ . It is noted that although the wave frequency increases with k , the increase or decrease of the phase velocity depends on the ranges of values of k as well as those of the parameters. Interestingly, for $k \ll 1$ and $k > 1$, the phase velocity approaches a constant value. While in the former case, the phase velocity remains smaller than c_s , in the latter, it may slightly exceed the same. However, a domain of k (< 1) exists corresponding to a wide range of values of the parameters where the phase velocity is close to the acoustic speed c_s . Thus, in contrast to typical acoustic waves (e.g., ion-acoustic wave), the thermoacoustic wave can propagate with sonic, subsonic or supersonic velocity. On the other hand, both the growth and the decay of the wave amplitude can occur in a wide range of values of k and the parameters. In this context, a purely growing mode or a purely damped mode can also exist when the collision frequency ν remains above or below a critical value. For example, given $q_\rho = 0.27$, $q_T = 0.34$, $\chi = 0.8$, $\Gamma = 3$ and $\mu = 0$, $\Im\omega \gtrless 0$ according to when $\nu \gtrless 0.005$ [See the thick and thin dotted lines of subplot (d)]. It is important to note that when the viscosity is absent ($\mu = 0$) in the medium, the growth/decay rate in both the cases reaches a maximum value within the domain $0 < k < 1$ having a cutoff at a higher $k > 1$ except the case with nonzero μ [See the dash-dotted line in subplot (d)].

III. NONLINEAR EVOLUTION OF SHOCKS

In the previous section II, we have seen that depending on the parameter values, the thermoacoustic interaction of density and temperature perturbations can lead to either the wave instability or damping. In this section, we consider this interaction effect and examine whether the linear perturbations, as they propagate and the nonlinear effects intervene, can develop into nonlinear compressive or rarefactive shocks with oscillatory or monotonic profiles. To this end, we derive an evolution equation for small amplitude shocks and study their characteristics in the parameter space.

In what follows, we are interested in the evolution of shocks in a frame that moves along the x -axis with a velocity close to the acoustic speed c_s . The wave can achieve this speed in a finite domain of k where k is not too small but can be smaller than unity and the pa-

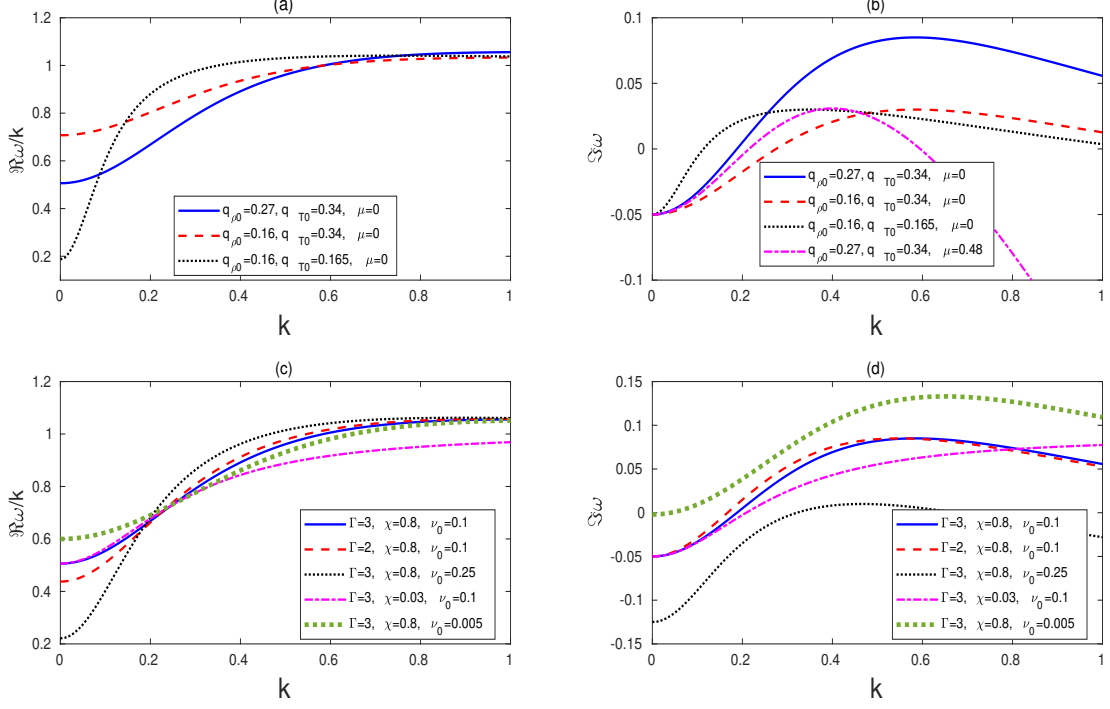


FIG. 1. The real [subplots (a) and (c)] and the imaginary [subplots (b) and (d)] parts of the wave frequency ω are plotted against the wave number k for different values of the parameters as in the legends to show the instability growth and decay rates of the wave. The fixed parameter values for the subplots [(a), (b)] and [(c), (d)], respectively, are $(\Gamma = 3, \chi = 0.8, \nu_0 = 0.1)$ and $(q_{\rho_0} = 0.27, q_{T_0} = 0.34, \mu = 0)$.

parameters satisfy the condition $q_{\rho}/(4\nu/\Gamma - 2q_T) < 1$ [cf. subplots (a) and (c) of Fig. 1]. Thus, in our reductive perturbation scheme the new space and time coordinates can be defined as [10]

$$\xi = \varepsilon(x - t) \text{ and } \tau = \varepsilon^2 t, \quad (9)$$

where ε is an expansion parameter that reflects the smallness of wave perturbations. We further assume that $\nu \sim \nu_0 \varepsilon$, $q_{\rho} \sim q_{\rho_0} \varepsilon$, and $q_T \sim q_{T_0} \varepsilon$, where ν_0 , q_{ρ_0} , and q_{T_0} are each of the order of unity. The dependent variables are expanded as

$$\begin{aligned} \rho &= 1 + \varepsilon \rho_1 + \varepsilon^2 \rho_2 + \varepsilon^3 \rho_3 + \dots, \\ v &= \varepsilon v_1 + \varepsilon^2 v_2 + \varepsilon^3 v_3 + \dots, \\ T &= 1 + \varepsilon T_1 + \varepsilon^2 T_2 + \varepsilon^3 T_3 + \dots, \\ q(\rho, T) &= \varepsilon^2 q_1 + \varepsilon^3 q_2 + \dots, \end{aligned} \quad (10)$$

where $q_1 \equiv q_{\rho_0} \rho_1 + q_{T_0} T_1 \sim \mathcal{O}(\varepsilon^2)$, $q_2 \equiv q_{\rho_0} \rho_2 + q_{T_0} T_2 \sim \mathcal{O}(\varepsilon^3)$ etc. are obtained by evaluating the first and higher order partial derivatives of $q(\rho, T)$ with respect to ρ and T at their equilibrium values.

Next, we substitute the new stretched coordinates from Eq. (9) and the expansion from Eq. (10) into Eqs. (1)-(3), and equate the coefficients of different powers of ε . In

the lowest order of ε , we obtain the following expressions for the first order perturbations.

$$v_1 = \rho_1, \quad T_1 = -\frac{\Gamma'}{2} \rho_1, \quad (11)$$

where $\Gamma' = 2(\nu_0 - q_{\rho_0}) / (2\nu_0/\Gamma - q_{T_0})$.

From the next order of ε , neglecting the secular terms by assuming $\partial/\partial\xi \gg 1/L$, where $1/L = \max\{\nu_0/\Gamma - q_{T_0}, q_{\rho_0}, \nu_0\}$, we obtain the following expressions for the second order perturbations in terms of first order quantities.

$$\frac{\partial v_2}{\partial\xi} - \frac{\partial \rho_2}{\partial\xi} = -\frac{\partial \rho_1}{\partial\tau} - 2\rho_1 \frac{\partial \rho_1}{\partial\xi}, \quad (12)$$

$$\frac{\partial T_2}{\partial\xi} - \frac{\partial v_2}{\partial\xi} + \frac{\partial \rho_2}{\partial\xi} = -\frac{\partial \rho_1}{\partial\tau} + \Gamma' \rho_1 \frac{\partial \rho_1}{\partial\xi} + \mu_0 \frac{\partial^2 \rho_1}{\partial\xi^2} - \nu_0 \rho_1^2, \quad (13)$$

$$-\frac{\partial T_2}{\partial\xi} = -\frac{\Gamma'}{2} \chi_0 \frac{\partial^2 \rho_1}{\partial\xi^2} + \frac{\Gamma'}{2} \frac{\partial \rho_1}{\partial\tau} + \frac{\Gamma'}{2} \rho_1 \frac{\partial \rho_1}{\partial\xi} - 2\frac{\nu_0}{\Gamma} T_2 + q_2. \quad (14)$$

After eliminating the second order perturbed quantities from Eqs. (12)-(14) and using the results, given by, Eq. (11), we obtain the following Bateman-Burgers or simply

the Burgers-like equation for thermoacoustic shocks in fluid complex plasmas.

$$\frac{\partial \rho}{\partial \tau} + A \rho \frac{\partial \rho}{\partial \xi} = B \frac{\partial^2 \rho}{\partial \xi^2} + D \rho^2, \quad (15)$$

where $\rho(\xi, \tau) \equiv \rho_1(\xi, \tau)$ and the coefficients of the non-linear convection, the diffusion and the nonlocal nonlinearity, respectively, are

$$A = \frac{3\Gamma' - 4}{\Gamma' - 4}, \quad B = \frac{\Gamma' \chi_0 - 2\mu_0}{\Gamma' - 4}, \quad D = \frac{2\nu_0}{\Gamma' - 4}. \quad (16)$$

We note that the nonlocal term $\propto D$ in Eq. (15) appears not only due to the particle collision but also a finite value of the heat capacity per particle and is modified by the thermal feedback of the medium to the density and thermal fluctuations. Furthermore, the nonlinearity in ρ appears due to the first order smallness of $\nu \sim \varepsilon$. However, a second order smallness of $\nu \sim \varepsilon^2$ could result into a linear term $\propto \rho$ in Eq. (15). So, the evolution dynamics of shocks with the linear term $D\rho$ should differ from that with the nonlinear term $D\rho^2$. Before going into the dynamics of shocks, it is imperative to investigate the nature of the coefficients A , B and D of Eq. (15) for different values of the parameters q_{ρ_0} , q_{T_0} , ν , Γ , χ and μ . The latter two, however, modify the coefficient of diffusion B only. Such an investigation is crucial not only to examine the existence of different kinds of shock solutions of Eq. (15) that the plasma medium can support but also to study their characteristics with the variation of parameters. Typically, the specific heat ratio Γ ranges in between 2 to 4. Also, we have $q_{\rho_0} \sim 0 - 0.4$, $q_{T_0} \sim 0 - 0.4$, $\chi_0 \sim 0 - 1$, $\mu_0 \sim 0 - 1$ and $\nu_0 \sim 0 - 1$ such that the condition $q_{\rho}/(4\nu/\Gamma - 2q_T) < 1$, as stated before, is fulfilled.

Figure 2 displays the profiles of A , B and D with respect to the collision frequency ν for different values of the other parameters. Here, we note that while the sign of A could be crucial for determining the existence of compressive or rarefactive shocks, that of D may characterize the emergence of instability or damping of non-linear shocks. Furthermore, the magnitudes of A , B and D should be finite in order to avoid any blow up solution of shocks. It is found that all the coefficients can assume exceedingly high values when the collision frequency outstrips its critical value ($\nu_c \sim 0.5$) and the thermal feedback (q_{T_0}) due to the temperature variation is relatively high [See the solid, dashed and dotted lines in subplots (a), (b) and (c)]. However, when the value of q_{T_0} is relatively low [See the dash-dotted lines in subplots (a), (b) and (c)], the coefficients A , B and D can be positive or negative depending on the ranges of values of ν_0 . Furthermore, B tends to assume positive values in the entire domain of ν_0 with an increasing value of the viscosity parameter μ . From the subplots (a) and (c), it is observed that in absence of the fluid viscosity and for a fixed value of χ , which characterizes the thermal diffusivity, the qualitative features of A and B are almost

the same except for their changes of signs and/or magnitudes with the variations of the parameters q_{ρ_0} , q_{T_0} and Γ . From the profiles of A , B and D it may be concluded that in order to have a finite shock solution the values of ν_0 may be restricted to lie in the interval $0 < \nu_0 \lesssim 0.5$. In the following section IV, we will consider these parameter regimes to investigate different kinds of shock solutions both analytically and numerically.

IV. SHOCK SOLUTION: ANALYTICAL AND NUMERICAL APPROACH

We employ the tanh expansion scheme [11] to obtain an approximate shock solution of Eq. (15) when the nonlocal nonlinearity is relatively small compared to the non-linear convection and the diffusion, i.e., $|D| \ll |A|$, $|B|$. We also numerically investigate the existence of different kinds of shock solutions and examine whether the qualitative features in both the cases agree in the same parameter space.

A. Analytical approach

We note that in absence of the particle collision ($\nu = 0$), Eq. (15) reduces to the known Burgers equation whose asymptotic shock solution is given by

$$\rho(\xi, \tau) = \frac{v_0}{A} \left[1 - \tanh \left\{ (\xi - v_0 \tau) \frac{v_0}{2B} \right\} \right], \quad (17)$$

where v_0 is the speed of the shock front and the imposed boundary conditions are ρ , ρ_{ξ} , $\rho_{\xi\xi} \rightarrow 0$ as $\xi \rightarrow \infty$. Such a shock profile has two layers which may be composed of compressive and/or rarefactive wave fronts. From Eq. (17), it is clear that the shocks can be compressive ($\rho > 0$) or rarefactive ($\rho < 0$) according to when the coefficient of the nonlinear convection A is positive or negative. We, however, skip the further analysis of this particular solution rather we look for a solution of Eq. (15) when the nonlocal nonlinearity is no longer negligible but small compared to those associated with A and B , i.e., we assume $|D| \ll |A|$, $|B|$. The case with $|D| \gtrsim |A|$, $|B|$ may result into blow up solutions which are physically inadmissible.

It is to be noted while various conservation laws, e.g., the conservation of total number of particles and the conservation of energy hold for the Burgers equation with $\nu = 0$, the same do not hold for Eq. (15) because of the nonlocal nonlinearity. So, either the wave energy grows leading to the instability or decays to exhibit the damping. It follows that a steady state solution with finite wave energy of Eq. (15) does not exist and thus, we look for an approximate solution of it. To this end we recast Eq. (15) as

$$\frac{\partial \rho}{\partial \tau} + A \rho \frac{\partial \rho}{\partial \xi} - B \frac{\partial^2 \rho}{\partial \xi^2} + \lambda \rho^2 = 0, \quad (18)$$

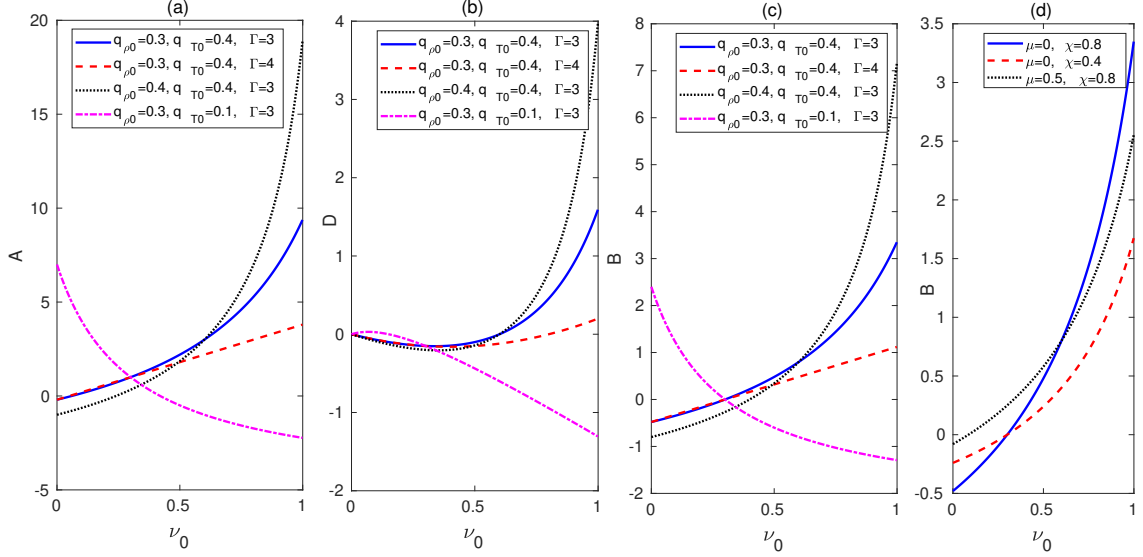


FIG. 2. The variations of the coefficients of Eq. (15) are shown in a domain of the collision frequency ν_0 for different values of the parameters that characterize the heat capacity (Γ), the thermal feedback due to density (q_{ρ_0}) and temperature (q_{T_0}) fluctuations, the thermal diffusion (χ) and the kinematic viscosity (μ) as in the legends. The fixed parameter values for the subplots [(a), (b), (c)] and (d), respectively, are ($\chi = 0.8$, $\mu = 0$) and ($q_{\rho_0} = 0.3$, $q_{T_0} = 0.4$, $\Gamma = 3$).

where $\lambda = -D$. We employ the tanh perturbation expansion scheme in which Eq. (18) can be treated as a perturbed equation with the small perturbation being $\propto \lambda$. So, it is reasonable to assume Eq. (17) as the unperturbed solution of Eq. (18) and a slow time dependence of the wave amplitude and velocity of the new solution due to the nonlocal term $\propto \lambda$. Thus, we define a new transformation ζ , retaining τ as is, as

$$\zeta = \frac{V}{B} [\xi - \phi(\tau)], \quad (19)$$

so that $\rho(\xi, \tau) \equiv \rho(\zeta, \tau)$ represents a localized solution of Eq. (18) which travels with a velocity $d\phi/d\tau$ having the characteristic width $W = B/V$ which plays the role of the wavelength. Here, we do not consider any time dependency of V in order to avoid any secular term $\propto \xi$. Using the transformation (19), Eq. (18) reduces to

$$\frac{\partial \rho}{\partial \tau} - \frac{V}{B} \frac{d\phi}{d\tau} \frac{\partial \rho}{\partial \zeta} + \frac{VA}{B} \rho \frac{\partial \rho}{\partial \zeta} - \frac{V^2}{B} \frac{\partial^2 \rho}{\partial \zeta^2} + \lambda \rho^2 = 0. \quad (20)$$

Next, we look for a solution in analogy with that of the Burgers equation with $\lambda = 0$ and use the similar boundary conditions, namely ρ , $\partial \rho / \partial \zeta$, $\partial^2 \rho / \partial \zeta^2 \rightarrow 0$ as $\zeta \rightarrow \pm \infty$. To this end, we introduce a variable $Y = \tanh(\zeta)$ for an infinite series expansion with τ -dependent coefficients and assume $\rho(\zeta, \tau) = S(Y, \tau)$. Thus, Eq. (20) gives

$$\frac{\partial S}{\partial \tau} + \lambda S^2 + \frac{V}{B} (1 - Y^2) \left[\frac{\partial S}{\partial Y} \left(-\frac{d\phi}{d\tau} + AS + 2VY \right) - V(1 - Y^2) \frac{\partial^2 S}{\partial Y^2} \right] = 0. \quad (21)$$

Based on the exact solution [Eq. (17)] of the conserved Burgers equation, we presume, as an ansatz, that the solution of Eq. (21) will take the form

$$S(Y, \tau) = G(\tau)(1 - Y) \left[1 + a_1(\tau)Y + a_2(\tau)Y^2 + a_3(\tau)Y^3 + a_4(\tau)Y^4 + a_5(\tau)Y^5 + \dots \right], \quad (22)$$

where $G(\tau)$ and $a_i(\tau)$, for $i = 1, 2, 3, \dots$, are unknown functions of τ , and the series in Y converges.

Substituting the ansatz (22) into Eq. (21) and equating the coefficients of Y^n , for $n = 0, 1, 2, \dots$, to zero one can obtain different expressions for $G(\tau)$, $\phi(\tau)$ and $a_i(\tau)$ with $i = 1, 2, 3, \dots$. First, to obtain the expressions for $G(\tau)$ and $\phi(\tau)$, we set $a_1(\tau) = a_2(\tau) = 0$. The lowest order of Y then gives

$$-\frac{VA}{B} G^2(\tau) + \lambda G^2(\tau) + G'(\tau) + \frac{V}{B} \frac{d\phi}{d\tau} G(\tau) = 0. \quad (23)$$

Next, looking for a solution of Eq. (23) for $G(\tau)$ that decays with time τ and hence the velocity $d\phi/d\tau$, we have

$$\frac{dG(\tau)}{d\tau} = -\lambda G^2(\tau), \quad (24)$$

$$\frac{d\phi}{d\tau} = AG(\tau). \quad (25)$$

Using the initial conditions $G(\tau) = 2V/A$ and $\phi(\tau) = 0$ at $\tau = 0$, and in analogy with the solution of the conserved Burgers equation, we obtain for $\lambda \neq 0$ the following solutions of Eqs. (24) and (25).

$$G(\tau) = \left(\lambda \tau + \frac{A}{2V} \right)^{-1}, \quad (26)$$

$$\phi(\tau) = \frac{A}{\lambda} \log \left(1 + \frac{2V\lambda}{A} \tau \right), \quad (27)$$

In particular, for $\lambda = 0$, Eqs. (24) and (25) give

$$G(\tau) = \frac{2V}{A}, \quad (28)$$

$$\phi(\tau) = v_0 \tau, \quad (29)$$

where $v_0 = 2V$. Here, for $\lambda = 0$, the exact solution can be written in terms of $S(Y, \tau) \equiv S(Y)$, i.e.,

$$S(Y) = \frac{v_0}{A} (1 - Y), \quad (30)$$

where $Y = \tanh(\zeta) = \tanh[(v_0/2B)(\xi - v_0\tau)]$ and the required boundary condition is $S(Y) \rightarrow 0$ as $Y \rightarrow 1$. The solution (30) completely agrees with the solution (17) of the conserved Burgers equation. From Eqs. (25) and (26) we note that both the amplitude $G(\tau)$ and the velocity $d\phi/d\tau$ of the thermoacoustic shock may either decay (damping) or grow (instability) with time depending on the values of the collision frequency below or above a critical value and those of q_{ρ_0} and q_{T_0} . Furthermore, depending on these values of the parameters, $G(\tau)$ can be either positive or negative implying the existence of either compressive or rarefactive shocks.

Next, the τ -dependent quantities $a_i(\tau)$ in the ansatz (22) are obtained successively from the higher orders of Y as follows:

$$a_3(\tau) = -\frac{1}{3} + \frac{1}{6V^2} (AV - B\lambda)G(\tau), \quad (31)$$

$$a_4(\tau) = a_3(\tau) + \frac{B\lambda}{12V^2} G(\tau), \quad (32)$$

$$a_5(\tau) = -\frac{8}{15} + \frac{1}{12V^2} (4AV - 3B\lambda)G(\tau) + \frac{A}{30V^3} (-Ac + B\lambda)G^2(\tau), \quad (33)$$

$$a_6(\tau) = a_5(\tau) + \frac{B\lambda}{9V^2} G(\tau) + \frac{B\lambda}{360V^4} (-9AV + 4B\lambda)G^2(\tau), \quad (34)$$

and so on. Finally, we obtain the following approximate shock solution of Eq. (15).

$$\rho(\xi, \tau) = \left(\lambda\tau + \frac{A}{2V} \right)^{-1} (1 - Y) \times [1 + a_3(\tau)Y^3 + a_4(\tau)Y^4 + \dots], \quad (35)$$

where

$$Y = \tanh \left[\frac{V}{B} (\xi - \phi(\tau)) \right]. \quad (36)$$

In Eq. (35), how many correction terms involving $a_i(\tau)$ are to be considered depends on the degree of smallness of the perturbation $\propto \lambda$. We, however, consider the terms upto $a_6(\tau)$. In particular, for $\lambda = 0$, we have $a_i(\tau) = 0$ with $i = 3, 4, 5, \dots$, for which the solution (17) is recovered. As said before, if the smallness of the collision frequency is taken to be the higher order of ε , than the first order, i.e., $\nu \sim \mathcal{O}(\varepsilon^2)$, then the nonlocal term in Eq. (15) appears as $D\rho$ instead of $D\rho^2$. In that case, the shock solution can have either exponential growth or exponential decay [11] which is significantly different from the present solution (35).

Before we analyze the characteristics of the shock solution, given by, Eq. (35), it is important to investigate the properties of the amplitude $G(\tau)$ and the velocity $d\phi/d\tau$ of the shock as well as the relative propagation distance $\phi(\tau)$ for a fixed time at which the shock may eventually damp away. The results are displayed in Fig. 3. It is evident that given fixed values of Γ , q_{ρ_0} and q_{T_0} when the collision frequency is below a critical value both the amplitude (> 0) and velocity of shocks decay with time [solid, dashed and dotted lines of subplots (a) and (c)]. Furthermore, in contrast to the decay rate of the velocity [subplot (c)], the decay rate of the wave amplitude can be lower (higher) with decreasing values of q_{ρ_0} (q_{T_0}). However, both the amplitude and the velocity can grow with time leading to the instability when ν_0 exceeds some critical value ν_c [See the dash-dotted lines in subplots (a) and (c)]. This critical value may differ due to a different set of other parameter values. Here, the instability occurs with positive amplitude of shocks. However, there may be some parameter regime, e.g., $\Gamma = 3$, $\chi = 0.8$, $\nu_0 = 0.1$, $q_{\rho_0} = 0.4$ and $q_{T_0} = 0.4$ at which even though $G(\tau)$ (< 0) decays, the velocity of shocks $d\phi/d\tau$ may increase with time. It follows that the rarefactive thermoacoustic shocks may exist with an increasing speed and can achieve its maximum value at finite distance and time before they damp away. On the other hand, subplot (b) shows that the relative propagation distance at which the shocks may eventually damp away can be different for different values of Γ , q_{ρ_0} and q_{T_0} . Here, one must note that while the values of both ϕ and $d\phi/d\tau$ increase, those of $G(\tau)$ decrease with decreasing values of Γ (not shown in the figure).

Figure 4 shows the profiles of the shock solution (35) for different values of the parameters that characterize the thermal feedback (q_{ρ_0} and q_{T_0}), kinematic viscosity (μ), thermal diffusivity (χ), particle collision (ν_0), and the heat capacity (Γ). We consider those parameter values for which $|D| < |A|$, $|B|$ [cf. Fig. 2] hold. It is seen that depending on the parameter regime, not only both the compressive and rarefactive shocks appear, a transition from oscillatory to monotonic shocks and vice versa can also occur. As they appear as double-layer shocks with multiple wave fronts [12], both the free and trapped particles can adjust themselves at any time to maintain the quasineutrality on each side of the propagating shocks. From the subplots (a) and (b) of Fig.

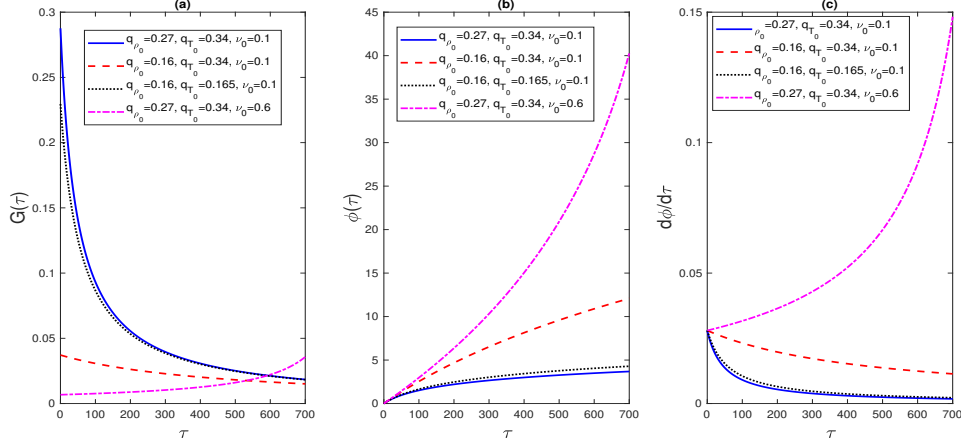


FIG. 3. The profiles of the amplitude $[G(\tau)]$, the relative propagation distance $[\phi(\tau)]$ and the velocity $(d\phi/d\tau)$ of thermoacoustic shocks are shown for fixed values of $\Gamma = 3$ and $V = 1$, and for different values of the other parameters as in the legends. While the solid, dashed and dotted lines correspond to the wave damping, the dash-dotted lines that to the instability of thermoacoustic shocks.

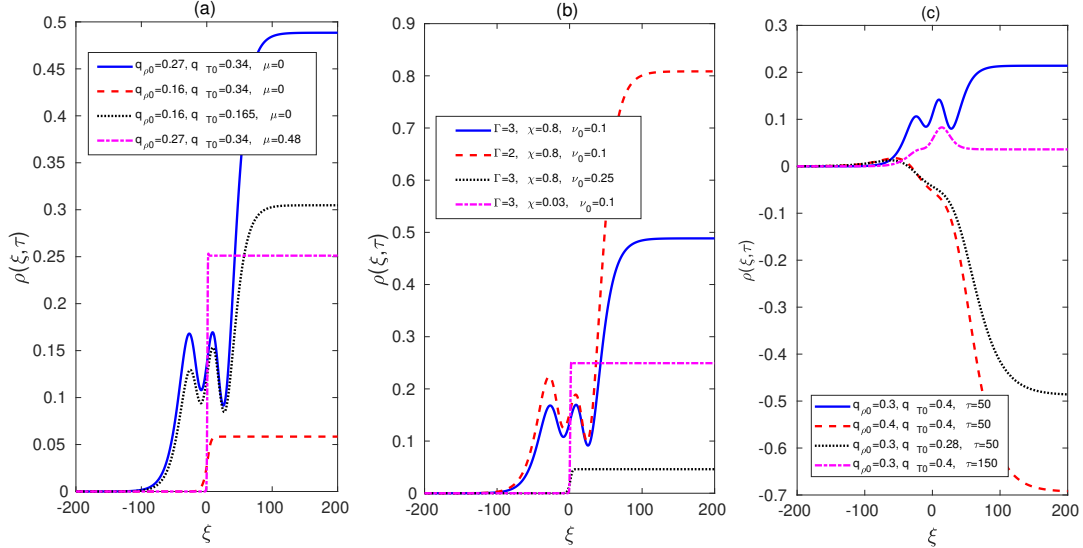


FIG. 4. The profiles of the asymptotic shock solution (35) are shown with the variations of parameters as in the legends. The transition from oscillatory to monotonic shocks occur due to the effects of (a) the kinematic viscosity (μ) as well as the thermal feedback associated with density (q_{ρ_0}) and thermal (q_{T_0}) fluctuations and (b) the thermal diffusion (χ) and the particle collision (ν_0). The fixed parameter values for the subplots (a) and (b), respectively, are ($\Gamma = 3$, $\chi = 0.8$, $\nu_0 = 0.1$) and ($q_{\rho_0} = 0.27$, $q_{T_0} = 0.34$, $\mu = 0$). Also, fixed are $\tau = 50$ and $V = 0.014$. Subplot (c) shows the existence of rarefactive shocks for a different set of parameter values as in the legend. The fixed parameter values in this case are $\Gamma = 3$, $\nu_0 = 0.1$ and $\mu = 0$.

4 it is evident that as the value of q_{ρ_0} is reduced keeping the other parameters fixed, an oscillatory shock with two wave fronts transits into a monotonic one with a reduced wave amplitude [See the solid and dashed lines in subplot (a)]. The shock profile remains monotonic in the interval $0.34 \lesssim q_{T_0} \lesssim 0.4$ and for fixed values of the other parameters, namely $q_{\rho_0} = 0.16$, $\Gamma = 3$, $\chi = 0.8$, $\nu_0 = 0.1$ and $\mu = 0$. In this regime, the monotonic shocks having amplitude ~ 0.03 and velocity ~ 0.02 will damp

away after traveling a finite distance $\phi \sim 1.3$ in time $\tau = 50$. Furthermore, such monotonic shocks again transit into an oscillatory one with an increased amplitude when the value of q_{T_0} is further reduced from $q_{T_0} = 0.34$ to $q_{T_0} = 0.165$ [See the dotted and dashed lines in subplot (a)]. The profile remains oscillatory in nature in the interval $0 < q_{T_0} < 0.34$ with $q_{\rho_0} = 0.16$, $\Gamma = 3$, $\chi = 0.8$, $\nu_0 = 0.1$ and $\mu = 0$. In this case, the oscillatory shocks having amplitude $\sim 0.04 - 0.13$ and veloc-

ity ~ 0.02 will damp in time $\tau = 50$ after a finite distance $\sim 1 - 1.3$. However, the oscillatory shock can also transit into a monotonic one with an increasing value of the coefficient of the kinematic viscosity μ (See the solid and dash-dotted line). On the other hand, subplot (c) shows that the shock profile can also become rarefactive with negative amplitude for slightly a different set of values of the parameters. Interestingly, this occurs when either the value of q_{ρ_0} is increased from $q_{\rho_0} = 0.3$ to $q_{\rho_0} = 0.4$ keeping other parameter values fixed with $q_{T_0} = 0.4$, $\Gamma = 3$, $\chi = 0.8$, $\nu_0 = 0.1$ and $\mu = 0$ or q_{T_0} is decreased from $q_{T_0} = 0.4$ to $q_{T_0} = 0.28$ with $q_{\rho_0} = 0.3$, $\Gamma = 3$, $\chi = 0.8$, $\nu_0 = 0.1$ and $\mu = 0$ (See the solid, dashed and dotted lines). It is also seen that as time goes on, the amplitude of the shock profile gets reduced (See the solid and dash-dotted lines) implying that the shock wave may be damped due to a small effect of the nonlocal nonlinearity. However, as mentioned before that even though the amplitude decays, the velocity of shocks can increase with time and achieve a maximum value before they damp away. In the following section IV B, we will investigate the existence and characteristics of different kinds of shocks numerically and examine any qualitative agreement with the analytical results.

B. Numerical approach

We numerically solve Eq. (15) using the Runge-Kutta scheme with an initial condition $\rho(\xi, 0) = 0.5[1 + \tanh(\xi/8)]$. The parameter values are considered as the same as for Fig. 4. We use 1000 grid points with the system scale size $L_\xi = 200$ and consider the pulse size $L_p < L_\xi$ so that the shock solutions exist. The results are displayed in Fig. 5. A good qualitative agreement of the results with those obtained from the analytical solutions are noted. Initially, the wave steepens with growing amplitude, however, as time progresses, it evolves into a steady state structure with wave fronts behind the shocks. The amplitude of the shocks so formed decays with time due to a small effect of the nonlocal nonlinearity. It is noted that the wave fronts behind the shock is ordered and the one with the maximum amplitude is nearest to the shock. From subplot (a) it is found that similar to Fig. 4, the wave steepening occurs with a small reduction of the value of q_{ρ_0} and as a result, the oscillatory shock transforms into a monotonic one with an increased amplitude (See the solid and dashed lines). The monotonic profile again transits back into the oscillatory one with almost the same profile as for the increased values of q_{ρ_0} and q_{T_0} (solid line) with a small reduction of q_{T_0} (See the dotted line). The similar qualitative features [in agreement with subplot (b) of Fig. 4] also occur by the effects of the other parameters, namely Γ , χ and ν_0 . It is to be noted that for a different set of parameter values at which the coefficients A , B and D of Eq.

(15) are significantly high or D becomes larger than or comparable to A and B , the shock solution evolves with growing amplitude and may eventually blow up after a finite time. This happens when the collision frequency exceeds a critical value and the values of q_{ρ_0} and/or q_{T_0} are relatively high.

V. CONCLUSIONS

Although the onset of thermoacoustic instability in complex plasmas was reported in previous studies in the linear regime, its consequences in the nonlinear regime have not been studied before. It is found that the temperature and density fluctuations characterizing the positive thermal feedback can lead to both monotonic and oscillatory double-layer shocks that can be damped due to small effect of the nonlocal nonlinearity associated with the particle collisions and nonreciprocal interactions of charged particles providing the thermal feedback. However, with the effects of the positive thermal feedback when the collision frequency exceeds a critical value, the shock wave amplitude can grow leading to the instability of shocks. A reductive perturbation technique is employed to show that the evolution of shocks can be described by the Burgers-like equation with nonlocal nonlinearity which can admit both compressive and rarefactive solutions. The analytical and numerical approaches show a good qualitative agreement of the characteristics of the thermoacoustic shocks in plasmas. The theory may be well applicable to systems like dusty plasmas, strongly coupled plasmas or complex plasma crystals as well as atmospheric fluids where the positive thermal feedback, necessary for the thermoacoustic instability, can occur due to inhomogeneities of equilibrium density and pressure. Furthermore, the thermoacoustic shocks so formed are able to transport particles and can thereby accelerate them in the medium.

DECLARATION OF COMPETING INTEREST

The authors declare that they have no known competing financial interests or personal relationships that could have appeared to influence the work reported in this paper.

ACKNOWLEDGMENTS

This work was partially supported by the SERB (Government of India) sponsored research project with sanction order no. CRG/2018/004475. G. Banerjee acknowledges support from UGC, Govt. of India, under the Dr. D. S. Kothari Post Doctoral Fellowship Scheme (PDF) with Ref. No. F.4-2/2006(BSR)/MA/18-19/0096.

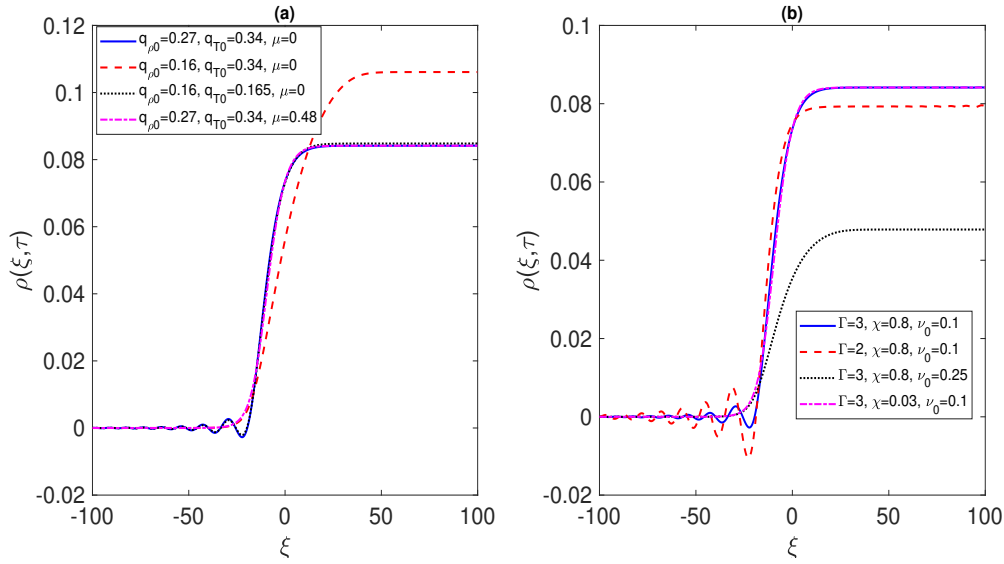


FIG. 5. The development of an initial profile $\rho(\xi, 0) = 0.5[1 + \tanh(\xi/8)]$ [Numerical solution of Eq. (15)] into shocks is shown after $\tau = 300$ for different sets of parameter values as in the legends and/or in Fig. 4.

-
- [1] F. Nicoud and T. Poinsot, *Combustion and Flame* **142**, 153 (2005).
- [2] G. Ghirardo, M. P. Juniper, and M. R. Bothien, *Combustion and Flame* **187**, 165 (2018).
- [3] V. Alekseev, M. Kuznetsov, Y. Yankin, and S. Dorofeev, *Journal of Loss Prevention in the Process Industries* **14**, 591 (2001).
- [4] A. Kiverin, I. Yakovenko, and M. Ivanov, *International Journal of Hydrogen Energy* **41**, 22465 (2016).
- [5] S. O. Yurchenko, E. V. Yakovlev, L. Couëdel, N. P. Kryuchkov, A. M. Lipaev, V. N. Naumkin, A. Y. Kislov, P. V. Ovcharov, K. I. Zaytsev, E. V. Vorob'ev, G. E. Morfill, and A. V. Ivlev, *Phys. Rev. E* **96**, 043201 (2017).
- [6] N. P. Kryuchkov, E. V. Yakovlev, E. A. Gorbunov, L. Couëdel, A. M. Lipaev, and S. O. Yurchenko, *Phys. Rev. Lett.* **121**, 075003 (2018).
- [7] S. Garai, A. Ghose-Choudhury, and S. Sain, *Physics of Plasmas* **27**, 103701 (2020), <https://doi.org/10.1063/5.0022676>.
- [8] T. Biwa, T. Takahashi, and T. Yazaki, *The Journal of the Acoustical Society of America* **130**, 3558 (2011), <https://doi.org/10.1121/1.3658444>.
- [9] T. Biwa, K. Sobata, S. Otake, and T. Yazaki, *The Journal of the Acoustical Society of America* **136**, 965 (2014), <https://doi.org/10.1121/1.4892782>.
- [10] S. E. Cousens, V. V. Yaroshenko, S. Sultana, M. A. Hellberg, F. Verheest, and I. Kourakis, *Phys. Rev. E* **89**, 043103 (2014).
- [11] W. Malfliet, *Journal of Physics A: Mathematical and General* **26**, L723 (1993).
- [12] A. P. Misra and S. Samanta, *Phys. Rev. E* **82**, 037401 (2010).